Geochemistry of shales of the Middle Buanji Group in the Kimani area, Southwest Tanzania: Implication to provenance and depositional environment

Almachius Mutasingwa[1], Michael Msabi[1], and Jagarlamudi Seetharamaiah[1]

[1]University of Dodoma

November 22, 2022

Abstract

Major and trace element proxies of the shale samples from the Middle Buanji Group of the Upper Paleoproterozoic (1.67 Ga) are reported in this paper to decipher the provenance and depositional environment in the study area. The analytical results of shales in the Middle Buanji Group indicates relatively low percentage of major oxides compositions such as; SiO_2 (38.84 – 54.26 %), Al_2O_3 (6.8 – 10 %), K_2O (2.22 – 3.04 %), TiO_2 (0.21 – 0.28 %) and CaO (0.15 – 0.51 %) and moderately high Fe_2O_3 (4.34 – 10.4 %) and P_2O_5 (1.62 – 2.01 %). The trace element composition of the analyzed shale samples displays wide concentration variation such as Mn (29 -19600 ppm), Ti (468 - 35600 ppm), P (370 – 4610 ppm), Ba (400 – 7730 ppm), and S (5 – 2350 ppm), V (130 – 290 ppm), Zn (5 – 100 ppm), Sr (40 – 160 ppm), As (2 – 70 ppm), and Cr (100 – 250 ppm). Measured proxies of major oxides Al_2O_3 /TiO_2 (10.86 to 15.31) and K_2O/Al_2O_3 (0.23 – 0.35). Variation of Cr concentrations in the shale samples indicates diverse source compositions in the study area ranging from; ultramafic, mafic, intermediate, to feldspar-rich rocks. The measured Mn values in shales have an average of 2527.65 ppm, and proxies of V/Cr: 0.65 – 1.7, V/ (V + Cr): 0.39 – 0.63, and CuO/Zn: 0.004 – 1.7 elements suggest that shales and dominant clay minerals (illite and chamosite) were deposited in marine environment under oxidizing conditions.

Hosted file

essoar.10507816.1.docx available at https://authorea.com/users/533902/articles/598333-geochemistry-of-shales-of-the-middle-buanji-group-in-the-kimani-area-southwest-tanzania-implication-to-provenance-and-depositional-environment

Geochemistry of shales of the Middle Buanji Group in the Kimani area, Southwest Tanzania: Implication to provenance and depositional environment

Almachius Mutasingwa*, Michael Msabi and Jagarlamudi Seetharamaiah

The University of Dodoma, College of Earth Sciences and Engineering, Department of Geology, P.O BOX 11090, Dodoma, Tanzania.

Email: almach86@yahoo.com; mmsabi@yahoo.com; jseetharamaiah@gmail.com

*Corresponding author: Almachius Mutasingwa; Email: almach86@yahoo.com

ORCID for corresponding author: 0000-0002-1427-397X

Key points

- The shales from the Middle Buanji Group indicates diverse composition in the range of ultramafic, mafic, intermediate and feldspar-rich rocks

- The shales and clay minerals are deposited in the marine environments under oxidizing conditions.

Abstract

Major and trace element proxies of the shale samples from the Middle Buanji Group of the Upper Paleoproterozoic (1.67 Ga) are reported in this paper to decipher the provenance and depositional environment in the study area. The analytical results of shales in the Middle Buanji Group indicates relatively low percentage of major oxides compositions such as; SiO_2 (38.84 – 54.26 %), Al_2O_3 (6.8 – 10 %), K_2O (2.22 – 3.04 %), TiO_2 (0.21 – 0.28 %) and CaO (0.15 – 0.51 %) and moderately high Fe_2O_3 (4.34 – 10.4 %) and P_2O_5 (1.62 – 2.01 %). The trace element composition of the analyzed shale samples displays wide concentration variation such as Mn (29 -19600 ppm), Ti (468 - 35600 ppm), P (370 – 4610 ppm), Ba (400 – 7730 ppm), and S (5 – 2350 ppm), V (130 – 290 ppm), Zn (5 – 100 ppm), Sr (40 – 160 ppm), As (2 – 70 ppm), and Cr (100 – 250 ppm). Measured proxies of major oxides Al_2O_3 /TiO_2 (10.86 to 15.31) and K_2O/Al_2O_3 (0.23 – 0.35). Variation of Cr concentrations in the shale samples indicates diverse source compositions in the study area ranging from; ultramafic, mafic, intermediate, to feldspar-rich rocks. The measured Mn values in shales have an average of 2527.65 ppm, and proxies of V/Cr: 0.65 – 1.7, V/ (V + Cr): 0.39 – 0.63, and CuO/Zn: 0.004 – 1.7 elements suggest that shales and dominant clay minerals (illite and chamosite) were deposited in marine environment under oxidizing conditions.

1

Introduction

The investigation of fine-grained sediments has been attracting the attention of researchers for the last thirty years because fine- grained terrigenous sediments such as shales and siltstones comprise

about 70% of the sedimentary record (Ahmad et al., 2014; Armstrong-Altrin et al., 2015; Bhuiyan et al., 2011; Jung et al., 2012; Tobia & Shangola, 2016). Fine-grained rocks such as shales are

typically deposited in lakes and lagoon deposits, river deltas, floodplains, and offshores; and occupy a large volume compared with other detrital sedimentary rocks (Tobia & Shangola, 2016). Several authors have used geochemical data of the shales to predict ancient sediments depositional conditions such as paleo redox conditions and provenance (Yarincik et al., 2000; Yang et al., 2004; Akinyemi et al., 2013; Ahmad et al., 2014; Armstrong-Altrin et al., 2015; Adeoye et al., 2020). This approach has been applied to fine-grained clastic sedimentary rocks which are dominantly deposited in different geological records of the basins for example Proterozoic (Kasanzu et al., 2008; Quasim et al., 2017; Ghaznavi et al., 2018; Rashid & Ganai 2018; Khan et al., 2019) and Mesozoic basins (Kasanzu et al., 2017; Tobia & Shangola, 2016). The geochemical signatures of shales are influenced by many complex factors such as the composition of source rocks, weathering conditions, transportation, digenesis, and metamorphism (Yarincik et al., 2000; Yang et al., 2004). Major elements such as K, Na, Ca, P, Ba, Mg, Sr, and Si are considered mobile and disperse more directly into detrital sediments thereby preserving a record of the source rock composition (Nesbitt, 1982; Middelburg et al., 1988; Hossain et al., 2017; Kasanzu et al., 2017). The major elements in the range of K, Ca, P, Sr, Mg, Si, and Ba are reported in this study.

The study area is dominated by different clastic sedimentary rocks ranging between brown to green shales, micaceous siltstone, dolomitic limestone, conglomerates, quartzite, and sandstone with variable thicknesses (Kasanzu et al., 2008; Manya, 2013; Kasanzu et al., 2017). From field observation, shales are categorized by reddish-brown, grey, and green/blue colours. Further, these shales are referred to as cupriferous shales (Manya, 2013) and/or shale-hosted copper (Mutasingwa et al., 2021) due to their green/blue colouration which has attracted copper exploitation through small-scale mining operations. The presence of colour variation in these shales (i.e., red, grey, and green/blue) remain unstudied in the Middle Buanji Group which could infer the prevailed conditions in their provenance and depositional environment. Kasanzu et al. (2017) reported the general provenance of the sediments in the whole Buanji Group, however, little is known for the shales in the Middle Buanji Group in terms of their provenance and depositional environment which led to their colour variation. The present study is therefore focused on the mineralogy and geochemistry of the shales of the Middle Buanji Group distributed in the Kimani area to understand their provenance and depositional conditions.

2 Geological Settings

The study area is located in the Mbarali district-Mbeya region, Southwest, Tanzania. It is bounded by latitudes 8° 48' 50.24" S and 8° 59' 11.15" S and longitudes 34° 1' 11.24" E and 34° 17' 23.86" E (Figure 1) as described on the Quarter Degree Sheet 246 (Harpum and Brown 1958). The area is dominated by the sedimentary rocks and lavas that overlie uncomfortably on the Proterozoic (2.1-

1.8 Ga) (Manya 2013; Kazimoto et al., 2015) Ubendian high-grade metamorphic rocks, gabbros, and granitic intrusive (Lenoir et al., 1994; Boven et al., 1999).

Stratigraphically, based on the lithological distribution the Buanji Group is subdivided into three sub-groups (Figure 2) which include the Lower, Middle, and Upper Buanji Groups (Harpum and Brown 1958; Manya, 2013). Kasanzu et al. (2017) reported the thickness of 245 m, 366 m, and 457 m, for Lower, Middle, and Upper Buanji Groups, respectively. The Lower Buanji Group contains rocks such as conglomerates comprised of pebbles of agate and jasper, red shales with intermittent quartzitic sandstones (Manya, 2013; Kasanzu et al., 2017). The Middle Buanji Group consists of brown and green shales, dolomitic limestone, conglomerates, quartzite, sandstone, and micaceous siltstone (Kasanzu et al., 2008; Manya, 2013: Kasanzu et al., 2017). Further, observation from fieldwork reports the presence of red or reddish-brown, grey, and blue shales in the Middle Buanji Group. The Middle Buanji shales are referred to as cupriferous shales (Manya, 2013) dominated by green colour (Figure 2) from which copper metal is locally exploited by small-scale miners. The Upper Buanji Group is characterized by greenish or greyish shales, mudstone, siltstone intercalated with sandstone and, the horizon of conglomerate and quartzite above which they are overlaid by dolomite with chert bands. The Upper Buanji division ends with effusive volcanism characterized by highly vesicular lavas on Chaufukwe Mountain (Manya, 2013; Kasanzu et al., 2017). Furthermore, some of the Middle Buanji Group rocks are rarely exposed due to the presence of thick soil cover in low lands, however, at the hillsides and tops, most of the rocks are well exposed. The whole area of the Buanji Group was tectonically affected by compressional deformation mechanisms that have led to various regional metamorphism and local thrusts (Harpum & Brown, 1958).

3 Materials and Methods

In this study, 16 shale samples were systematically collected from the outcrops and channel cuttings based on their colour i.e., green, red, grey shales, and locations are given in Figure 1. The collected shale samples with grey and red colours were found in a single sedimentary succession within the Middle Buanji Group. All sixteen (16) samples were crushed to 2 mm size and powdered to -75 mesh by using Jaw crusher and Swing Mill, respectively. About 0.5 g of each powdered sample was pressed onto the white caps, then covered with transmitted paper

film at both ends for analysis. Major and trace elements were analyzed on X-Ray Florescence Spectrometer (XRF; MiniPal4 and Nilton Model) (Geological Survey of Tanzania) with ± 0.1 ppm and ± 0.01 ppm detection limit, respectively. The copper (Code: CS28054) was used as standard material for the analysis for which the precision and accuracy was 6.78%. Standard procedures for the determination of the major and trace elements concentrations using the X-Ray Fluorescence (XRF) were followed as reported by Petruk (2000).

4 Results

4.1 Major and Trace elements

The results of major elements of the Middle Buanji Group shale samples are given in Table 1. The results showed significant compositional variations, of which silica (SiO_2) ranged from 38.84 to 59.6 wt%, (average = 49.31 wt %). The shale samples also contained CuO (0.39-32.2 wt%, average = 12.26 wt%), Al_2O_3 (0.1 – 10 wt% average = 8.02 wt%), Fe_2O_3 (4.23 – 10.4 wt% average = 7.31 wt%), K_2O (2.19 – 3.04 wt% average = 2.59 wt%), CaO (0.15 – 0.78 wt%, average = 0.34 wt%) and ZrO_2 (0.14 – 0.26 wt%, average = 0.19 wt%). The conversion of CuO to elemental composition (Cu metal) shows the variation of copper concentrations among red shales (0.31 wt %), grey shales (0.35 – 10.9 wt%, average = 5.2 wt %) and green shales (0.31 – 25.7 wt%, average = 13.17 wt %). The trace element composition of the analyzed shale samples displayed wide variations in terms of concentrations, such as Mn (290 – 19600 ppm), Ti (3560 – 4680 ppm), P (3700 – 4610 ppm), and Ba (130 – 7730 ppm) and S (10 – 3050 ppm) (Table 1) Based on proxies of major oxides Al_2O_3 /TiO_2 (10.86 to 15.31; average 12.82) and K_2O/Al_2O_3 (0.23 – 0.35, average = 0.29). The measured Mn values in shales have an average of 2527.65 ppm, and proxies of V/Cr (0.65 – 1.7; average = 1.1), V/ (V + Cr) (0.39 – 0.63; average = 0.5), and CuO/Zn (0.004 – 1.7, average = 0.22) (Table 2).

5 Discussion

5.1 Major element

The major oxide concentrations of sixteen (16) samples and ratios of the oxides are given in Table

1. The summary of the average major element oxides (wt%) data for the studied samples was compared to average shales published worldwide as reported by Pettijohn (1957), Gromet et al., , (1984), Turekian et al. (1961), and Taylor and McLennan (1985). Results revealed that most of the shale had a relatively low percentage of major elements such as; SiO_2 (38.84 – 54.26 %), Al_2O_3 (6.8 – 10 %), K_2O (2.22 – 3.04%), TiO_2 (0.21 – 0.28 %) and CaO (0.15 – 0.51%) and moderately high Fe_2O_3 (4.34 – 10.4 %) and P_2O_5 (1.62 – 2.01 %). More of the K_2O in the clay minerals are sourced from the weathering of muscovite/biotite

(Dayal & Varma 2017) from the pre-existing parent materials (Galán, 2006). The presence of the K_2O in the shale samples suggests a decrease of micas (i.e., muscovite and biotite) minerals as an ideal source during which weathering of K- bearing rocks release K^+ into the shales. Shale materials with low CaO and MgO compositions indicate merely not associated with carbonate or dolomitization (Okunlola & Idowu, 2012). The reported low CaO composition (0.15 – 0.51 %; average = 0.28 %) of the shale samples indicate that they are poorly associated with carbonates. Samples with a low composition of P_2O_5 indicate depleted with an accessory phase such as apatite (phosphate-bearing) and monazite (Ramasamy et al., 2007; Okunlola & Idowu, 2012). The P_2O_5 values recorded in this study range between 1.62 – 2.01 % with an average of 1.68 % which is higher as compared to reported P_2O_5 average values 0.15 – 0.2% (Pettijohn 1957; Turekian et al., 1961; Gromet et al., 1984; Okunlola & Idowu, 2012; Taylor & McLennan, 1985) (Table 2). Therefore, the high P_2O_5 composition in this study suggests the presence of several amounts of accessory minerals associated with shales. Similarly, the XFR results of the shales from this study reported higher P (3700 – 4610 ppm) (Table 1) which affirms the presence of pseudomalachite as a major accessory mineral (Mutasingwa et al., 2021). Shales in this study have shown a composition of SiO_2 and Al_2O_3 to be of an average of 45.65 % and 8.04 %, respectively. Nesbitt (1984) reported that the chemical content of the deposited sediments is the characteristic of the degree of chemical weathering. Thus, during weathering cation with large ionic radius (such as Al, Mg, Cs, etc) remain intact in the source rocks while cation with small radius (such as K, Na, Ca) are easily dissolved, transported, and deposited together with newly formed sediments (Nesbitt, 1982; Kasanzu et al., 2017). The rate at which the small ionic radius is dissolved, transported, and deposited from their precursor rocks defines the degree of weathering of a particular geological environment (Condie, 1993). The reported low alumina concentration (average = 8.04 %) in this study is probably as a result of low to an intermediate degree of weathering prevailed in their provenance of which did not incorporate more of Al into the sediments because of its immobile nature. This is in agreement with Chemical Index Alteration (CIA) value reported in the study area ranging between 73 – 81; average = 76) indicating an intermediate degree of weathering (Kasanzu et al., 2017). In addition, Han et al. (2020) worked on the comparative study of the shales between two wells in the Lower Cambrian Shale Formations in Northern Guizhou, South China from which reported Al_2O_3 content of 8.73 % and 13.28 % in the two wells with respective CIA values between 35.43 and 71.48; average = 60.94, and 58.48 and 80.67; average = 70.71 which indicating lower alumina content correspond to the lower CIA values and vice versa.

5.2 Paleo-provenance characteristics

The presence of minerals, such as illite and chamosite (Chlorite-group mineral) is an indication of older formation and occurs in restricted shallow marine environments characterized by $> 20^O C$ of warm-bottom water as an ideal formation condition for these clay minerals (Net et al., 2002). These minerals have been

reported in the study area by (Mutasingwa et al., 2021). The immobile trace elements such as Ti, Zr, and Ni are used as geochemical proxies to demarcate the provenance of the sediments (Floyd et al., 1989; Hayashi et al., 1997). The TiO_2 against Zr binary diagram indicates that most of the samples plot in the intermediate source provenance field (Figure 3). Al_2O_3/TiO_2 ratios are useful in deciphering the provenance of the sediments with the granitic to a mixture of granitic/basaltic composition (Amajor, 1987). The Al_2O_3/TiO_2 ratios in felsic rocks generally range between 10 and 100 and < 20 for mafic rocks (Hayashi et al., 1997; Kasanzu et al., 2017; Sindhuja et al., 2019). On the other hand, Archean and Proterozoic shales have high Al_2O_3/TiO_2 ratios of an average of 50 and 31, respectively, which reflect felsic sources (Hayashi et al., 1997). The provenance of the clastic rocks can be deduced from the Al_2O_3/TiO_2 ratios whereby Al_2O_3/TiO_2 for most of them ranges from 3 to 8 for mafic rocks, 8 to 21 for intermediate rocks, and 21 to 70 for felsic igneous rocks (Hayashi et al., 1997; Adeoye et al., 2020). Results from this study indicate that Al_2O_3/TiO_2 ratio ranges between 10.86 and 15.31 (average = 12.82) (Table 1), thus suggesting intermediate source rocks. It has been revealed from elsewhere that the K_2O/Al_2O_3 ratio can also be used as an indicator to infer the early sediments' original composition. The K_2O/Al_2O_3 ratios of the clay minerals and feldspars vary between $0.0 - 0.3$ and $0.3 - 0.9$, respectively, (Cox et al., 1995). In this study, the K_2O/Al_2O_3 ratios range from $0.23 - 0.35$ which indicates the presence of feldspars and clay-rich rocks.

The use of trace elements to infer sediments provenance has been studied by various researchers, (e.g., Piper & Calvert, 2009; Adegoke et al., 2014; Adeoye et al., 2020). Trace elements such as chromium (Cr) have been useful due to its variable redox states which describe its mobility behavior in the environments (Fendorf, 1995; Ball & Nordstrom, 1998) either as immobile (Cr^{3+}) or mobile (Cr^{4+}) (Oze et al., 2004). The presence of chromium (i.e., Cr^{3+}) in the depositional environments is a result of the dissolution of host minerals (i.e., chromite, $FeCr_2O_4$). The dissolution is controlled by several factors, such as mineral abundance and reactivity, water pH, and the redox state of an individual element (Middelburg et al., 1988; Aiuppa et al., 2000).

However, chromite weathers slowly under ambient conditions and require strong oxidant such as MnO_2 or H_2O_2 to oxidize Cr^{3+} (immobile) to Cr^{4+} (mobile) (Oze et al., 2007; Hao et al., 2017). Oxidation of trace elements such as Fe, Mn, Cr, Cu, Mo, and Re significantly increases their solubility rate in the surface waters along with isotopic fractionation (Hao et al., 2017). Most of the immobile elements are transported and deposited in the sedimentary environments as a solution and organic complexes, adsorbed, precipitated, and co-precipitated, organic solids, and crystalline sediments (Gibbs, 1973). Gibbs (1973; 1977), further reported that the Cr element is deposited in the fine-grained sediments such as shales, as detrital particle or adsorbed-ion particle both of which are controlled by source area geology.

High concentration of Cr > 150 ppm and Ni > 100 ppm in the sediments are

indicative of the ultramafic source rocks (Garver et al., 1996) and low Cr concentration suggests mafic source rocks (Wrafter & Graham, 1989). Out of sixteen (16) analyzed samples in this study, eleven (11) samples showed the Cr concentrations ranging between 150 – 250 ppm which suggests ultramafic rocks as a possible source. Only five (5) samples showed Cr concentrations ranging between 100 –140 ppm (Table 1). Nevertheless, mafic rocks have been noted to contribute high concentrations of Cr and V in clay-rich sediments (Hossain et al., 2017). In this regard, the results of Cr (100 – 140 ppm; average = 126 ppm) and V (130 – 290 ppm; average = 185.29 ppm) reported in this study, might have sourced from mafic rocks.

5.3 Paleoredox conditions

The geochemistry of manganese in sedimentary environments is dominated by the redox control of its speciation and higher oxidation states (Mn^{3+} and Mn^{4+}) occurring as insoluble oxyhydroxides in oxic environments whereby the lower oxidation state (Mn^{2+}) is more soluble in anoxic conditions (Calvert & Pedersen, 1996). Mn^{2+} is released during weathering of mafic silicates under anoxic conditions (Van Cappellen et al., 1998) and incorporated into clays in the form of adsorbed-ion particles (Gibbs, 1973). Mn metal has been useful as an indicator of bottom water conditions due to its sensitivity to redox changes. Different types of shales are grouped based on their Mn contents and paleo-oxygenated conditions. The type 1 shales contain Mn of an average of 1000 ppm indicating oxic conditions, type 2 and 3 shales has 150 – 310 ppm Mn signifying anoxic, and type 4 shales with an average of 75 ppm Mn showing highly reduced bottom water conditions (Yang et al., 2004). Further, other studies have reported Mn concentration in shales of an average of 56,000 ppm indicating oxic conditions (Quinby-Hunt & Wilde, 1994), and Mn < 260 ppm showing anoxic (Pi et al., 2014; Tobia & Shangola, 2016). Results from this study indicate that Mn concentration ranges between 290 – 19600 ppm, (average, Mn = 2527.65 ppm) suggesting oxic conditions for the deposited shales in the Middle Buanji Group. The Mn value reported in this study is far higher (Mn = 2527.65 ppm) above its crustal abundance of about 1000 ppm (Yaroshevsky, 2006), and occurs as an oxyhydroxides in both pelagic sediments deposited in the deep ocean and surficial continental margin environments (Goldberg & Arrhenius, 1958; Calvert & Pedersen 1996). Further, a recent study by Adeoye et al. (2020) reported that the presence of high Mn concentrations in the shales suggests a marine depositional environment under oxic conditions.

Redox-sensitive transition group elements have been useful in understanding various fundamental geochemical processes (Huang et al., 2015). Vanadium (V), in particular, has been considered a key redox indicator to decipher and interpret past surface environments. Vanadium has been considered widely due to its occurrence in diverse redox states, such as -1, 0, +2, +3, +4, and +5, the highest oxidation states are mostly used (i.e., V^{3+}, V^{4+}, V^{5+}) (Huang et al., 2015; Shaheen et al., 2019). Vanadium (V^{5+}) is the most mobile element

(Shaheen et al., 2019), whereby, vanadium (V^{3+}) is insoluble and easily oxidized to vanadium (V^{4+}) or vanadium (V^{5+}) under low levels of oxygen (Imtiaz et al., 2015). Solubility of vanadium species is controlled by the pH and Eh conditions (Taylor &Van Staden, 1994), whereby, V^{5+} is stable in oxic environments at low pH, V^{4+} is stable under suboxic conditions, and vanadium (V^{3+}) is found in anoxic environment of pH up to 10 (Sadiq, 1988; Huang et al., 2015). However, in both oxic and anoxic environments vanadium can be soluble if the pH is higher up to 8. Weathering processes play a significant role in the oxidation of vanadium species such as V^{3+} and V^{4+} to V^{5+} resulting in major V mobilization into the sediment (Yang et al., 2014). These distinct chemical signatures of V are preserved in sedimentary marine rocks which make it a potential proxy for establishing paleo-redox and paleo-productivity conditions (Tribovillard et al., 2006; Anbar & Rouxel 2007).

To infer the paleo-redox characteristics of the deposited sediments, the V/Cr ratio has been considered as a key paleo-oxygenated indicator (Dill, 1986; Dill et al., 1988; Adegoke et al., 2014; Ekoko et al., 2019). Most studies have indicated that values of V/Cr > 4.5, $2 - 4.25$, < 2, respectively, represent anoxic, dysoxic, more oxidizing depositional conditions (Dill et al., 1988; Jones & Manning, 1994; Adegoke et al., 2014; Adeoye et al., 2020). The results of V/Cr ratios in this study ranges between $0.65 - 1.7$; average $= 1.1$ (Table 1) suggesting oxidizing conditions. Under relatively oxidizing conditions heavy metals like copper are leached from the porous country rocks and precipitated as sulfides/phosphates when the reduced beds like green shales are encountered. Thus, the environment of deposition is alkaline with low oxidation potential indicating shales deposited in most shallow-water seas. Moreover, (Hallberg, 1976), put forward Cu/Zn ratio as redox parameters to infer their depositional conditions. Okunlola & Idowu (2012) studied Cu/Zn ratios of the shales and clay-stone from the Bida Basin (Nigeria) and suggested that Cu/Zn ratios ranging between ~0.03 to 1.15, and ~1.7 to 2.0 respectively, indicate an oxidizing condition in which the shales were deposited. The results from this study have recorded Cu/Zn ratios between 0.004 and 1.7; average $= 0.22$ suggesting oxidizing depositional conditions.

6 Conclusions

Mineralogy and Geochemistry of the shales from the Middle Buanji Group were studied to constrain the depositional environment in the Kimani area and the following has been concluded:

1. The proxies for major element oxides Al_2O_3/TiO_2 (10.86 to 15.31, average $= 12.82$) and K_2O/Al_2O_3 ($0.23 - 0.35$, average $= 0.3$) indicate an intermediate, and feldspars and clay-rich rocks, respectively, as the ideal source that has contributed to the shale composition. Also, the Cr concentrations recorded in this study range between $150 - 250$ ppm and $100 - 140$ ppm, indicating ultramafic and mafic rocks as the source materials for the deposited shales, respectively. Therefore, the shales in the study area orig-

inated from mixed sources which include ultramafic, mafic, intermediate, feldspar, and clay-rich rocks.

2. The reported Mn values (290 – 19600 ppm; average = 2527.65 ppm), V/Cr (0.65 – 1.7; average

= 1.1), V/ (V + Cr) (0.39 – 0.63; average = 0.5) and Cu/Zn (0.004 to 1.7, average = 0.22) proxies for the shales in this study are suggesting marine depositional environment restricted under oxidizing conditions.

Data availability Statement

Data set of this research can be obtained from this paper. All other data supporting the discussion and conclusion can be obtained within tables in this paper.

Acknowledgment

Conflict of interest

On behalf of all authors, the corresponding author states that there is no conflict of interest in this work.

References

Adegoke, A. K., Abdullah, W. H., Hakimi, M. H., Sarki-Yandoka, B. M., Mustapha, K. A., & Aturamu, A. O., (2014). Trace elements geochemistry of kerogen in Upper Cretaceous sediments, Chad (Bornu) Basin, northeastern Nigeria: Origin and paleo-redox conditions. *Journal of African Earth Science,* 100(2014), 675–683. https://doi.org/10.1016/j.jafrearsci.2014.08.014

Adeoye, J. A., Akande, S. O., Adekeye, O. A., & Abikoye, V. T., (2020). Geochemistry and paleoecology of shales from the Cenomanian-Turonian Afowo formation Dahomey Basin, Nigeria: Implication for provenance and paleoenvironments. *Journal of African Earth Science,* 169, 1–38. https://doi.org/10.1016/j.jafrearsci.2020.103887

Ahmad, A. H. M., Noufal, K. N., Masroor, A. M., & Khan, T., (2014). Petrography and geochemistry of Jumara Dome sediments, Kachchh Basin: Implications for provenance, tectonic setting and weathering intensity. Chinese Journal Geochemical, 33(1), 9–23. https:/doi/org/10.1007/s11631-014-0656-4

Aiuppa, A., Allard, P., D'Alessandro, W., Michel, A., Parello, F., Treuil, M., & Valenza, M., (2000). Mobility and fluxes of major, minor and trace metals during basalt weathering and groundwater transport at Mt. Etna volcano (Sicily). *Geochimica et Cosmochimica Acta*, 64(11), 1827–1841. https://doi.org/10.1016/S0016-7037(00)00345-8.

Akinyemi, S. A., Adebayo, O. F., Ojo, O. A., Fadipe, O. A., & Gitari, W. M., (2013). Mineralogy and Geochemical Appraisal of Paleo-Redox Indicators in Maastrichtian Outcrop Shales of Mamu Formation, Anambra Basin, Nigeria. *Journal of Natural Sciences Research,* 3(10), 48–65.

Amajor, L. C., (1987). Major and trace element geochemistry of Albian and Turonian shales from the Southern Benue trough, Nigeria. *Journal of Natural Sciences Research,* 6(5), 633–641.

Anbar, A. D., & Rouxel, O., (2007). Metal stable isotopes in paleoceanography. *Annual Review of Earth and Planetary Sciences.* https://doi.org/10.1146/annurev.earth.34.031405.125029

Armstrong-Altrin, J. S., Machain-Castillo, M. L., Rosales-Hoz, L., Carranza-Edwards, A., Sanchez-Cabeza, J. A., & Ruíz-Fernández, A. C., (2015). Provenance and depositional history of continental slope sediments in the Southwestern Gulf of Mexico unraveled by geochemical analysis. *Continental Shelf Research*, 95, 15–26.

Ball, J. W., & Nordstrom, D. K., (1998). Critical evaluation and selection of standard state thermodynamic properties for chromium metal and its aqueous ions, hydrolysis species, oxides, and hydroxides. *Journal of Chemical & Engineering Data*, 43(6), 95–918. https://doi.org/10.1021/je980080a

Bhuiyan, M. A. H., Rahman, M. J. J, Dampare, S. B, & Suzuki, S., (2011). Provenance, tectonics and source weathering of modern fluvial sediments of the Brahmaputra-Jamuna River, Bangladesh: Inference from geochemistry. *Journal of Geochemical Exploration,* 111(3), 113–137.

Boven, A., Theunissen, K., Sklyarov, E., Klerkx, J., Melnikov, A., Mruma, A., & Punzalan, L., (1999). Timing of exhumation of a high-pressure mafic granulite terrane of the Paleoproterozoic Ubende belt (West Tanzania). *Precambrian Research,* 93(1), 119–137.

Calvert, S. E., & Pedersen, T. F., (1996). Sedimentary geochemistry of manganese: Implications for the environment of formation of manganiferous black shales. *Ecology Geology*, 91(1), 36–47. https://doi.org/10.2113/gsecongeo.91.1.36

Cox, R. D., & Cullers, R. L., (1995). The influence of sediment recycling and basement composition on evolution of mudrock chemistry in the southwestern United States. *Geochimica et Cosmochimical Acta*, 59(14), 2919–2940.

Dayal, A. M., & Varma, A. K., (2017). Exploration Technique. In Shale Gas: Exploration and Environmental and Economic Impacts, 65–93.

Dill, H., (1986). Metallogenesis of Early Paleozoic Graptolite Shales from the

Graefenthal Horst (Northern Bavaria-Federal Republic of Germany). *Economic Geology*, 81 (4), 889–903. https://doi.org/10.2113/gsecongeo.81.4.889.

Dill, H., Teschner, M., & Wehner, H., (1988). Petrography, inorganic and organic geochemistry of Lower Permian carbonaceous fan sequences ("Brandschiefer Series") - Federal Republic of Germany: Constraints to their paleogeography and assessment of their source rock potential. *Chemical Geology*, 67(3–4), 307–325.

Ekoko, E. B., Philip, F., Emile, E., Isaac, K. N., Salomon, B. B., Daniel, F. A., & Bessa, A. Z. E., (2019). Geochemical characteristics of shales in the Mamfe Basin, South West Cameroon: Implication for depositional environments and oxidation conditions. *Journal African Earth Science*, 149(August), 131–142. https://doi.org/10.1016/j.jafrearsci.2018.08.004

Fendorf, S. E., (1995). Surface reactions of chromium in soils and waters. *Geoderma* 67(1–2), 55–71. https://doi.org/10.1016/0016-7061(94)00062-F

Floyd, P. A., Winchester, J. A., & Park, R. G., (1989). Geochemistry and tectonic setting of Lewisian clastic metasediments from the Early Proterozoic Loch Maree Group of Gairloch, NW Scotland. *Precambrian Resource,* 45(1–3), 203–214).

Galán, E., (2006). Chapter 14 Genesis of Clay Minerals. *Development Clay Science,* 1, 1129–1162.

Garver, J. I., Royce, P. R., & Smick, T. A., (1996). Chromium and nickel in shale of the Taconic foreland: A case study for the provenance of fine-grained sediments with an ultramafic source. *Journal of Sedimentary Resource*, 66(1), 100–106. https://doi.org/10.1306/D42682C5-2B26-11D7-8648000102C1865D

Ghaznavi, A. A., Khan, I., Quasim, M. A., & Ahmad, A. H. M., (2018). Provenance, tectonic setting, source weathering and palaeoenvironmental implications of Middle-Upper Jurassic rocks of Ler dome, Kachchh, western India: Inferences from petrography and geochemistry. Chemical Der Erde, 78(3), 356–371. https://doi.org/10.1016/j.chemer.2018.06.002

Gibbs, R. J., (1973). Mechanisms of Trace Metal Transport in Rivers. Science, 180(4081), 71–73.

Gibbs, R. J., (1977). Transport phases of transition metals in the Amazon and Yukon Rivers. *Geological Society America Bulletin*, 88(6), 829–843. https://doi.org/10.1130/0016-7606(1977)88<829:TPOTMI>2.0.CO;2

Goldberg, E. D, & Arrhenius, G. O. S., (1958). Chemistry of Pacific pelagic sediments. *Geochimimica Cosmochimica Acta,* 13(2–3). https://doi.org/10.1016/0016-7037(58)90046-2

Gromet, L. P., Haskin, L. A., Korotev, R. L., & Dymek, R. F., (1984). The North American shale composite: Its compilation, major and trace element characteristics. *Geochimimica Cosmochimica Acta,* 48(12), 2469–2482.

Hallberg, R., (1976). A geochemical method for investigation of palaeoredox conditions in sediments. *Ambio Special Report*, 4, 139–147.

Han, S., Zhang, Y., Huang, J., Rui, Y., & Tang, Z., (2020). Elemental geochemical characterization of sedimentary conditions and organic matter enrichment for lower cambrian shale formations in northern guizhou, South China. *Mineral*, 10(9), 1–21. https://doi.org/10.3390/min10090793

Hao, J., Sverjensky, D. A., & Hazen, R. M., (2017). Mobility of nutrients and trace metals during weathering in the late Archean. *Earth Planet Science Letters*, 471(August), 148–159. https://doi.org/10.1016/j.epsl.2017.05.003

Harpum, J., & Brown, P., (1958). Geology of Chimala. Quarter Degree Sheet 246. *Geological Survey of Tanganyika.*

Hayashi, K. I., Fujisawa, H., Holland, H. D., & Ohmoto, H., (1997). Geochemistry of 1.9 Ga sedimentary rocks from northeastern Labrador, Canada. *Geochimica Cosmochimica Acta*, 61(19), 4115–4137.

Hossain, H. M. Z., Kawahata, H., Roser, B. P., Sampei, Y., Manaka, T., & Otani, S., (2017). Geochemical characteristics of modern river sediments in Myanmar and Thailand: Implications for provenance and weathering. *Geochemistry*, 77(3), 443–458. https://doi.org/10.1016/j.chemer.2017.07.005

Huang, J., Huang, F., Evans, L., & Glasauer, S., (2015). Vanadium: Global (bio)geochemistry. *Chemical Geololgy,* 1–68. https://doi.org/10.1016/j.chemgeo.2015.09.019

Imtiaz, M., Rizwan, M. S., Xiong, S., Li, H., Ashraf, M., Shahzad, S. M., Shahzad, M., Rizwan, M., & Tu, S., (2015). Vanadium, recent advancements and research prospects: *A review Environment International*, 80(April 2019), 79–88. https://doi.org/10.1016/j.envint.2015.03.018

Jones, B., & Manning, D. A. C., (1994). Comparison of geochemical indices used for the interpretation of palaeoredox conditions in ancient mudstones. *Chemical Geology*, 111(1–4), 111–129.

Jung, H. S., Lim, D., Choi, JY., Yoo, H. S., Rho, K. C., & Lee, H. B., (2012). Rare-earth element compositions of core sediments from the shelf of the South Sea, Korea: Their controls and origins. *Continental Shelf Research*, 48, 75–86.

Kasanzu, C. H., Maboko, M. A. H., & Manya, S., (2017). Geochemistry and Sm-Nd systematics of the 1.67 Ga Buanji Group of southwestern Tanzania: Paleoweathering, provenance and paleo-tectonic setting implications. Geoscience Frontier, 8(5), 1025–1037.

Kasanzu, C. H., Maboko, M. A. H., & Manya, S., (2008). Geochemistry of fine-grained clastic sedimentary rocks of the Neoproterozoic Ikorongo Group, NE Tanzania: Implications for provenance and source rock weathering. *Precambrian Research*, 164, 201–213.

Kazimoto, E. O., Schenk, V., & Appel, P., (2015). Granulite-facies metamorphic events in the northwestern Ubendian Belt of Tanzania: Implications for the

Neoarchean to Paleoproterozoic crustal evolution. *Precambrian Research*, 256, 31–47.

Kent, C. C., (1993). Chemical composition and evolution of the upper continental crust: Contrasting results from surface samples and shales. *Chemical Geology,* 104, 1–37.

Khan, Z., Quasim, M. A., Amir, M., & Ahmad, A. H. M., (2019). Provenance, tectonic setting, and source area weathering of Middle Jurassic siliciclastic rocks of Chari Formation, Jumara Dome, Kachchh Basin, Western India: Sedimentological, mineralogical, and geochemical constraints. *Geological Journal*, 55(5), 3537–3558. https://doi.org/10.1002/gj.3612

Lenoir, J. L., Liégeois, J. P., Theunissen, K., & Klerkx, J., (1994). The Palaeoproterozoic Ubendian shear belt in Tanzania: geochronology and structure. *Journal African Earth Science,* 19(3), 169–184.

Manya, S., & Maboko, M. A. H., (2003). Dating basaltic volcanism in the Neoarchaean Sukumaland Greenstone Belt of the Tanzania Craton using the Sm-Nd method: Implications for the geological evolution of the Tanzania Craton. *Precambrian Research,* 121(1–2), 35–45. https://doi.org/10.1016/S0301-9268(02)00195-X

Manya, S., (2013). Geochemistry and U – Pb zircon dating of the high-K calc-alkaline basaltic andesitic lavas from the Buanji Group, south-western Tanzania. *Journal of African Earth Science*, 86, 107–118.

Middelburg, J. J., Van der Weijden, C. H., & Woittiez, J. R. W., (1988). Chemical processes affecting the mobility of major, minor and trace elements during weathering of granitic rocks. *Chemical Geology,* 68(3–4), 253–273. https://doi.org/10.1016/0009-2541(88)90025-3

Mutasingwa, A., Msabi, M., Jackson, N., & Jagarlamudi, S., (2021). Mineralogy and Geochemistry of Shale-Hosted Copper of the Middle Buanji. *Tanzania Journal of Sci*ence, *47*(1), 378–389.

Nesbitt, H. W., & Young, G. M., (1982). Early Proterozoic climates and plate motions inferred from major element chemistry of lutites. 299, 715–717.

Nesbitt, H. W., & Young, G. M., (1984). Prediction of some weathering trends of plutonic and volcanic rocks based on thermodynamic and kinetic considerations. *Geochimica Cosmochimica Act*, 48(7), 1523–1534. https://doi.org/10.1016/0016-7037(84)90408-3

Net, L. I., Alonso, M. S., & Limarino, C. O., (2002). Source rock and environmental control on clay mineral associations, Lower Section of Paganzo Group (Carboniferous), Northwest Argentina. *Sedimentary Geology,* 152(3–4), 183–199.

Okunlola, O. A., & Idowu, O., (2012). The geochemistry of claystone-shale deposits from the Maastritchian Patti formation, Southern Bida basin, Nigeria.

Journal of Earth Science Research, 16(2), 57–67.

Oze, C., Bird, D. K., & Fendorf, S., (2007). Genesis of hexavalent chromium from natural sources in soil and groundwater. *Proceedings of National Academic Science United States of America*, 104(16), 6544–6549. https://doi.org/10.1073/pnas.0701085104

Oze, C., Fendorf, S., Bird, D. K., & Coleman, R. G., (2004). Genesis of hexavalent chromium from natural sources in soil and groundwate. *American Journal of Science*, 304(1), 67–101. https://doi.org/10.2475/ajs.304.1.67

Pettijohn, F., (1957). Sedimentary rocks (3rd ed.)

Pi, D. H., Jiang, S. Y., Luo, L., Yang, J. H., & Ling, H. F., (2014). Depositional environments for stratiform witherite deposits in the Lower Cambrian black shale sequence of the Yangtze Platform, southern Qinling region, SW China: Evidence from redox-sensitive trace element geochemistry. *Palaeogeography, Palaeoclimate, Palaeoecology,* 398, 125–131. https://doi.org/10.1016/j.palaeo.2013.09.029

Piper, D. Z., & Calvert, S. E., (2009). A marine biogeochemical perspective on black shale deposition. *Earth Science Review*, 95(1–2), 63–96. https://doi.org/10.1016/j.earscirev.2009.03.001

Quasim, M. A., Khan, I., & Ahmad, A. H. M., (2017). Integrated petrographic, mineralogical, and geochemical study of the upper Kaimur Group of rocks, Son Valley, India: Implications for provenance, source area weathering and tectonic setting. *Journal of Geological Society India*, 90(4), 467–484. https://doi.org/10.1007/s12594-017-0740-6

Quinby-Hunt, M. S., & Wilde, P., (1994). Thermodynamic zonation in the black shale facies based on iron-manganese-vanadium content. *Chemical Geology*, 113(3–4), 297–317. https://doi.org/10.1016/0009-2541(94)90072-8

Ramasamy, N., Madhavaraju, J., Nagendra, R., Armstrong-Altrin, J. S., & Moutte, J., (2007). Geochemistry of Neoproterozoic shales of the Rabanpalli Formation, Bhima Basin, Northern Karnataka, southern India: Implications for provenance and paleoredox conditions. *Review Mexicana de Cienc Geol*, 24(2), 150–160.

Rashid, S. A., & Ganai, J. A., (2018). Depositional environments, provenance and paleoclimatic implications of Ordovician siliciclastic rocks of the Thango Formation, Spiti Valley, Tethys Himalaya, northern India. *Journal of Asian Earth Science,* 157, 371–386.

Sadiq, M., (1988). Thermodynamic solubility relationships of inorganic vanadium in the marine environment. *Marine Chemistry*, 23(1–2), 87–96. https://doi.org/10.1016/0304-4203(88)90024-2

Shaheen, S. M., Alessi, D. S., Tack, F. M. G., Ok, Y. S., Kim, K. H., Gustafsson, J. P., Sparks, D. L., & Rinklebe, J., (2019). Redox chemistry of vanadium in soils

and sediments: Interactions with colloidal materials, mobilization, speciation, and relevant environmental implications. *Advances in Colloid and Interface Science,* 265, 1–13. https://doi.org/10.1016/j.cis.2019.01.002

Sindhuja, C. S., Khelen, A. C., & Manikyamba, C., (2019). Geochemistry of Archean–Proterozoic shales, Dharwar Craton, India: Implications on depositional environment. *Geological Journal,* 54(5), 2759–2778.

Taylor, M. J. C., & Van Staden, J. F., (1994). Spectrophotometric determination of vanadium(IV) and vanadium(V) in each other's presence Review. An 119(6), 1263–1276. https://doi.org/10.1039/AN9941901263

Taylor, S. R., & McLennan, S. M., (1985). The continental crust: its composition and evolution. Blackwell Oxford 312.

Tobia, F. H., & Shangola, S. S., (2016). Mineralogy, geochemistry, and depositional environment of the Beduh shale (Lower Triassic), Northern Thrust Zone, Iraq. *Turkish Journal of Earth Science*, 25(4), 367–391.

Tribovillard, N., Algeo, T. J., Lyons, T., & Riboulleau, A., (2006). Trace metals as paleoredox and paleoproductivity proxies: An update. *Chemical Geology*, 232(1–2), 12–32. https://doi.org/10.1016/j.chemgeo.2006.02.012

Turekian, K. K., & Hans, K. W., (1961). Distribution of the Elements in Some Major Units of the Earth's Crust. *Geological Society American Bulletin* , 72(February), 175–192.

Van Cappellen, P., Viollier, E., Roychoudhury, A., Clark, L., Ingall, E., Lowe, K., & Dichristina, T., (1998). Biogeochemical cycles of manganese and iron at the oxic-anoxic transition of a stratified marine basin (Orca Basin, Gulf of Mexico). *Environmetal Science Technology*, 3*2*(19), 2931–2939. https://doi.org/10.1021/es980307m

Wrafter, J. P., & Graham, J. R., (1989). Ophiolitic detritus in the Ordovician sediments of South Mayo, Ireland. *Journal of Geological Society* (London), 146(2), 213–215.

Yang, J., Jiang, S., Ling, H., Feng, H., Chen, Y., & Chen, J., (2004). Paleoceangraphic significance of redox-sensitive metals of black shales in the basal Lower Cambrian Niutitang Formation in Guizhou Province, South China. *Proceedings of Natural Science*, 14(2), 152–157.

Yarincik, K. M., Murray, R. W., Lyons, T. W., Peterson, L. C., & Haug, G. H., (2000). Oxygenation history of bottom waters in the Cariaco Basin, Venezuela, over the past 578,000 years: Results from redox-sensitive metals (Mo, V, Mn, and Fe). *Paleoceanography,* 15(6), 593–604. https://doi.org/10.1029/1999PA000401

Yaroshevsky, A. A., (2006) Abundances of chemical elements in the Earth's crust. *Geochemistry International*, 44(1), 48–55. https://doi.org/10.1134/S001670290601006X
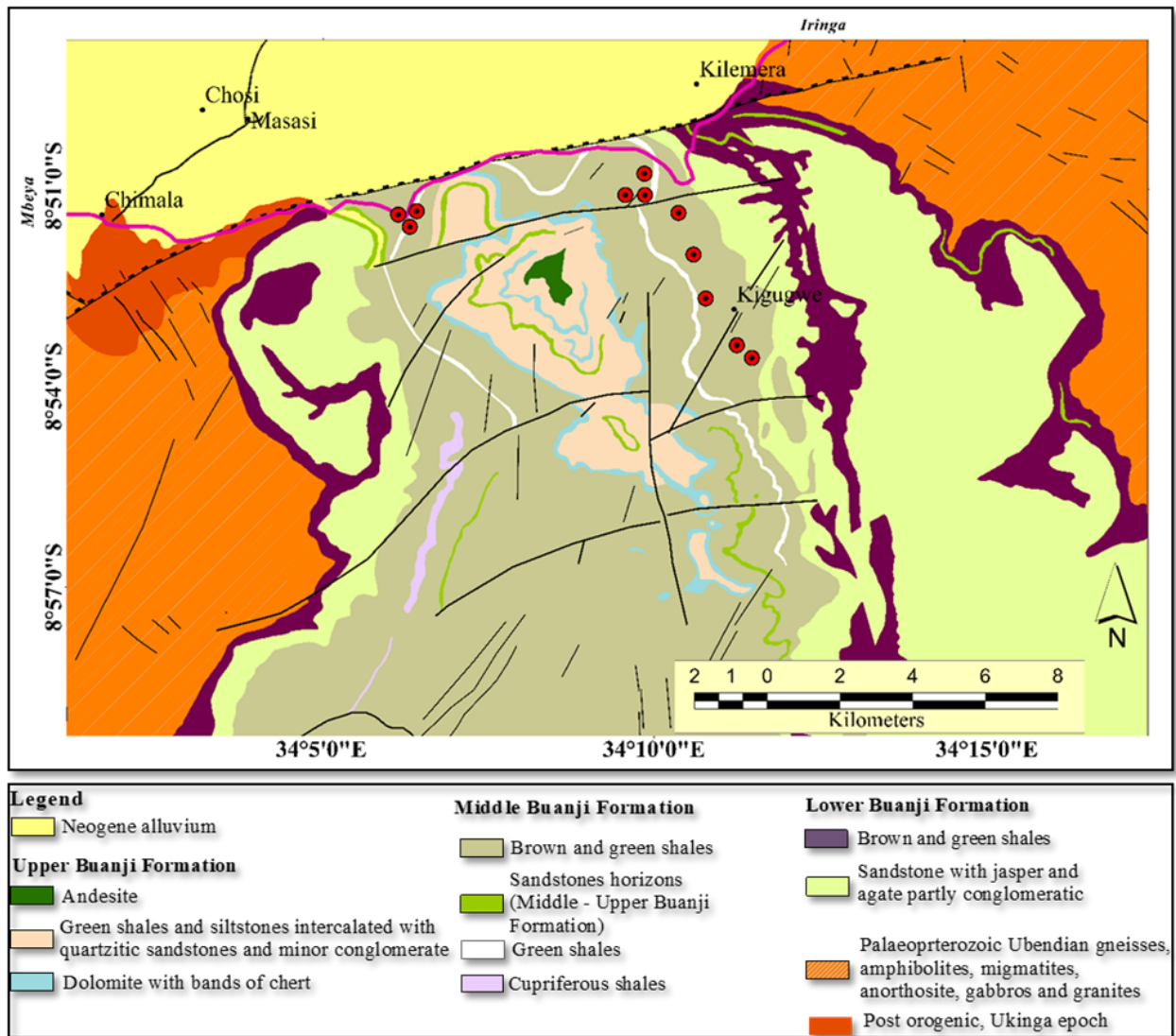
Figure 1. Showing geology and the locations of the collected samples (Solid lines indicates the fault lines and red spot indicate sample point) in the modified Buanji Group geological map (adopted from Mutasingwa et al., 2021).

Figure 2. A stratigraphic section showing Buanji Group (adopted from Mutasingwa et al., 2021).

Table 1. Major (wt %) and trace (ppm) elements distribution of the shale from Middle Buanji Group.

@ >p(- 32) * >p(- 32) * >p(- 32) * >p(- 32) * >p(- 32) * >p(- 32) * >p(- 32) * >p(- 32) * >p(- 32) * >p(- 32) * >p(- 32) * >p(- 32) * >p(- 32) * >p(- 32) * >p(- 32) * >p(- 32) * @

Sample ID

&

C1

&

C2

&

17

C3

&

C4

&

C5

&

C6

&

C7

&

C8

&

C9

&

C10

&

C11

&

C12

&

C13

&

C14

&

C15

&

C16

SiO2

&

47.35

&

38.84

&

54.26

&

43.62

&

51.87

&

47.35

&

51.34

&

52.4

&

51.21

&

44.42

&

52

&

46.82

&

52.14

&

44.16

&

45.89

&

52.4

Al2O3

&

8.8

&

8.1

&

9.8

&

9.5

&

7.8

&

7.8

&

10

&

9.5

&

9.5

&

6.8

&

9

&

7.6

&

7.9

&

7.4

&

8.7

&

8.4

Fe2O3

&

8.91

&

10.4

&

5.83

&

9.51

&

8.89

&

8.59

&

6.09

&

7.48

&

4.34

&

6.59

&

6.48

&

8.93

&

4.61

&

4.75

&

6.48

&

9.49

CaO

&

0.29

&

0.21

&

0.3

&

0.33

&

0.15

&

0.37

&

0.17

&

0.33

&

0.16

&

0.51

&

0.31

&

0.3

&

0.39

&

0.43

&

0.3

&

0.27

K2O

&

2.81

&

2.22

&

3.01

&

2.19

&

2.76

&

2.42

&

2.89

&

3.04

&

2.49

&

2.3

&

2.85

&

2.37

&

2.31

&

2.28

&

2.83

&

2.72

ZrO2

&

0.16

&

0.18

&

0.22

&

0.18

&

0.26

&

0.21

&

0.17

&

0.19

&

0.2

&

0.14

&

0.2

&

0.2

&

0.19

&

0.17

&

0.18

&

0.19

CuO

&

2.12

&

10.63

&

1.74

&

9.86

&

0.44

&

2.71

&

17.87

&

0.39

&

26.62

&

28.03

&

8.5

&

10.02

&

32.23

&

12.82

&

0.39

&

10.63

Trace elements (ppm)

& & & & & & & & & & & & & & & &

Ti

&

4230

&

4010

&

3830

&

4140

&

4140

&

4110

&

4680

&

4000

&

3780

&

3560

&

3980

&

4180

&

3720

&

3630

&

3770

&

4240

Mn

&

1460

&

19600

&

2870

&

2220

&

1520

&

2650

&

460

&

290

&

710

&

2030

&

2440

&

1450

&

940

&

1580

&

2220

&

530

S

&

1970

&

12

&

5

&

280

&

670

&

190

&

200

&

5

&

1110

&

2350

&

3050

&

9

&

230

&

1420

&

220

&

8

P

&

3970

&

4270

&

4130

&

4290

&

3740

&

3960

&

4610

&

4090

&

4430

&

3830

&

3900

&

4390

&

3700

&

4120

&

4040

&

4050

V

&

150

&

280

&

220

&

230

&

150

&

190

&

290

&

190

&

190

&

170

&

190

&

180

&

130

&

170

&

210

&

210

Zn

&

70

&

100

&

20

&

90

&

90

&

80

&

100

&

30

&

80

&

100

&

20

&

100

&

60

&

70

&

12

&

5

Sr

&

160

&

90

&

60

&

60

&

60

&

50

&

90

&

40

&

90

&

60

&

50

&

50

&

50

&

50

&

50

As

&

20

&

60

&

10

&

2

&

11

&

20

&

70

&

10

&

20

&

40

&

40

&

5

&

20

&

30

&

30

&

6

Cr

&

230

&

250

&

140

&

150

&

160

&

180

&

220

&

220

&

130

&

190

&

130

&

190

&

130

&

100

&

190

&

190

Ba

&

2520

&

1310

&

640

&

2250

&

840

&

700

&

1830

&

510

&

1880

&

7730

&

510

&

740

&

1290

&

920

&

410

&

400

Calculated element and element oxides (wt %)

& & & & & & & & & & & & & & &

Cu

&

0.31

&

8.49

&

1.39

&

10.39

&

7.9

&

0.35

&

14.3

&

1.69

&

21.3

&

22.4

&

6.79

&

8

&

25.7

&

10.2

&

0.31

&

8.49

TiO2

&

0.25

&

0.24

&

0.23

&

0.25

&

0.25

&

0.25

&

0.28

&

0.24

&

0.23

&

0.21

&

0.24

&

0.25

&

0.22

&

0.22

&

0.23

&

0.25

MnO

&

8.84

&

0.66

&

4.5

&

5.82

&

8.49

&

4.87

&

28.07

&

44.52

&

18.19

&

6.36

&

5.29

&

8.9

&

13.74

&

8.17

&

5.82

&

24.36

P2O5

&

1.73

&

1.86

&

1.8

&

1.87

&

    1.63

&

    1.73

&

    2.01

&

    1.79

&

    1.93

&

    1.67

&

    1.7

&

    1.92

&

    1.62

&

    1.79

&

    1.76

&

    1.77

Table 2. Comparing the average chemical composition of the Buanji shales to the published average shales

@ >p(- 12) * >p(- 12) * >p(- 12) * >p(- 12) * >p(- 12) * >p(- 12) * >p(- 12) * @

    Elements

&

Average Shale Middle Buanji Group

&

Average shale Bida Basin (Okunlola and Idowu, 2012)

&

Average shale

&

Turekan & Wedephol (1961)

&

PAAS (Taylor & McLennan, 1985)

&

NASC *(*Gromet et al., **1984)**

& & &

(Pettijohn, 1957)

& & &

SiO2

&

45.65

&

62.26

&

58.1

&

58.5

&

62.40

&

64.82

TiO2

&

0.23

&

1.74

&

0.6

&

0.77

&

0.99

&

0.8

Al2O3

&

8.04

&

16.88

&

15.4

&

15

&

18.78

&

17.05

Fe2O3

&

6.9

&

3.75

&

6.9

&

4.72

&

7.18

&

5.7

MgO

&

-

&

0.16

&

2.4

&

2.5

&

2.19

&

2.83

CaO
&

0.28
&

0.05
&

3.1
&

3.1
&

1.29
&

3.51

Na2O
&

-
&

0.06
&

1.3
&

1.3
&

1.19
&

1.13

K2O
&

2.44
&

1.39
&

3.2
&

3.1
&

3.68
&

3.97

P2O5
&

1.68
&

0.08
&

0.2
&

0.16
&

0.16
&

0.15

Al2O3/TiO2 &

12.82

&

9.70

&

25.67

&

19.48

&

18.96

&

21.31

K2O/Al2O3

&

0.29

&

0.08

&

0.21

&

0.21

&

0.2

&

0.23

V/(V+Cr)

&

0.5

& & & & &

CuO/Zn

&

0.22

&

0.12

& & & &
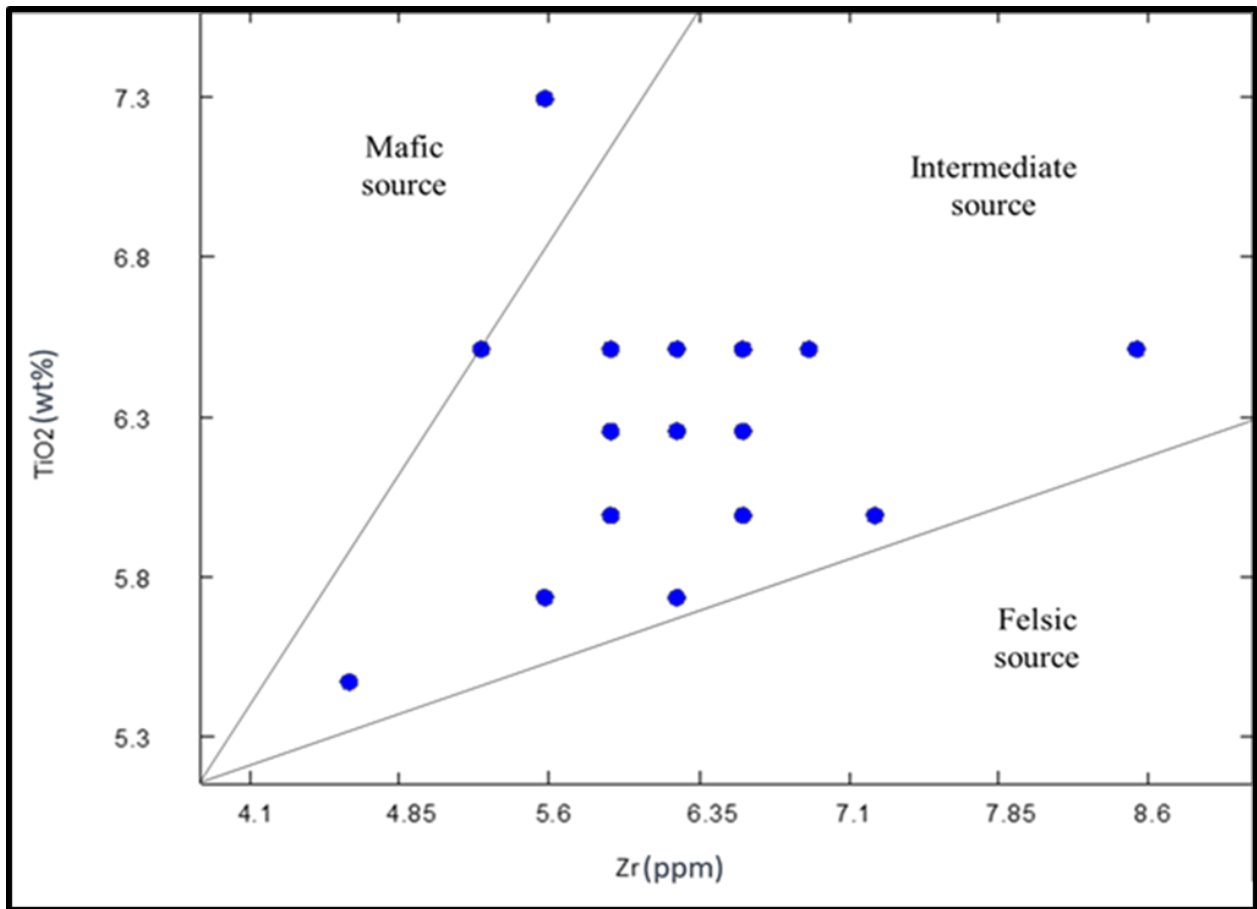
Figure 3. TiO$_2$ against Zr binary diagram reflecting the intermediate source provenance for the studied shales (Plotted are the normalized values) (modified

after Hayashi et al., 1997 and Sindhuja et al., 2019).